CHAPTER 5

TiO_2 nanoparticles induced omphalocele in chicken embryo: Transcriptomic evidences on distruption of Wnt signaling pathway

TiO_2 nanoparticles induced omphalocele in chicken embryo: Evidences on distruption of Wnt signaling pathway

INTRODUCTION

Nanomaterials (NMs) are widely used in specific biomedicine fields for treating, diagnosing, monitoring, controlling, and repairing biological systems at the molecular level (Moghimi *et al.*, 2005; Gunter Oberdörster, 2010; Shvedova & Kagan, 2010). The recent inventory of NMs has shown that the nano-encapsulates, silver and TiO_2 NPs are the most often used NMs (Peters *et al.*, 2014; Smolkova *et al.*, 2015). TiO_2 NPs are widely used in number of applications, such as a white pigment in paint, ceramics, as a food additive, in food packaging material, in sunscreens, in cosmetic creams and as a component of surgical implants. They are also broadly used in the environmental decontamination of air, water and soil by destruction of pesticides (Besov *et al.*, 2010; Choi *et al.*, 2006; H. Shi *et al.*, 2013; Tran & Webster, 2009).TiO_2 NPs are also under investigation as potential photosensitizers for use in photodynamic therapy (PDT) (Szaciłowski *et al.*, 2005). Similarly, nanopreparations with TiO_2 NPs are intensively evaluated as a novel therapy for dermatologic diseases, including acne vulgaris, atopic dermatitis, hyperpigmented skin lesions, etc (Wiesenthal *et al.*, 2011).

TiO_2 occurs naturally as anatase, rutile and brookite mineral forms, of which rutile and anatase are most common. Rutile is considered as a more inert form, whereas anatase is an active form of TiO_2 with the greater toxic potential than TiO_2 rutile (Nemmar *et al.*, 2013; H. Shi *et al.*, 2013). Their characteristics can be modified by several methods to improve their functionality and stability. In the connection, TiO_2 nanorods can be doped

with iron to increase their photocatalytic activity (Nemmar *et al.*, 2008). Further, surface modification such as coating, influences the activity of TiO_2 NPs (Liang *et al.*, 2006). Although the small size and subsequent larger surface area of TiO_2 ENPs make them applicable for various biomedical and commercial applications, it also renders them biologically more active leading to unexpected consequences on interaction with biological systems. With the increasing production and use of TiO_2 ENPs in products, occupational and environmental exposure to these ENPs will also increase. All these apprehensions have generated a public debate over understanding and managing the potential adverse effects of engineered TiO_2 ENPs on human health and the environment. The potential adverse health effects of TiO_2 have been investigated in different experimental investigations (Christie *et al.*, 1963; Lee *et al.*, 1986) and in some epidemiological studies (Chen & Fayerweather, 1988). On the basis of these studies TiO_2 was considered to be less toxic, biologically inactive and physiologically inert (Ferin & Oberdörster, 1985). With nanotechnology emerging, the use of TiO_2 is more pronounced in the form of TiO_2 NPs because of its versatile properties. Cytotoxic potential of TiO_2 NPs is well documented in a variety of cell lines. Oxidative DNA damage and apoptosis in HepG2 cells and in human epidermal cells (Shukla *et al.*, 2013), apoptosis and/or necrosis in human astrocytoma (astrocytes-like) U87 cells (Lai *et al.*, 2008) and mitochondrial dysfunction in BRL 3A cells (Hussain *et al.*, 2005) are some of the recent reports on cytotoxicity of TiO_2 NPs. Toxicity of TiO_2 NPs based on difference in their size has been documented in nematodes (Li *et al.*, 2012) and earthworm (Hu *et al.*, 2010). The ability of TiO_2 NPs to produce reactive oxygen species and surface charge are the reasons accredited for their toxicity (Gupta *et al.*, 2016; Shukla *et al.*, 2013). Several

engineered nanometals including TiO_2 NPs have been known to persist in the food chain and move across trophic levels resulting in various forms of toxic manifestations (Gupta *et al.*, 2016). Hence, their effect on reproductive performance and embryonic development cannot be ignored. Accelerated hatching of larvae and deformed embryos in zebrafish (Clemente *et al.*, 2014) and histopathological changes in juvenile carp (Linhua *et al.*, 2009) are few evidences on TiO_2 NPs induced toxicity on embryonic and post-hatch development. Hatching inhibition and malformation of embryos of Abalone have been reported following TiO_2 NPs exposure (Zhu *et al.*, 2011).

TiO_2 NPs can enter human body through inhalation, ingestion and dermal route (Günter Oberdörster *et al.*, 2005) and accumulate in liver, kidney, lungs, heart and brain. Maternal exposure of TiO_2 NPs during prenatal period affects gene regulating brain development and impacts hippocampal region of the offspring (Mohammadipour *et al.*, 2014). These reports provide compelling evidences on systemic and developmental toxicity of TiO_2 NPs but questions related to their mode of action are unanswered. Hence, chicken embryo was chosen as an experimental model in our study to assess the impact of TiO_2 NPs on embryonic development.

MATERIALS AND METHODS

Spectroscopic characterization

Protein-nanoparticle interaction was identified by Fourier transform infrared (FTIR) spectra (PerkinElmer spectrum 65 series, PerkinElmer, Inc., MA, USA). Sample was prepared by making pellet of 1.5 to 2 mg of sample mixed with 200 mg KBr (AR, Sigma, USA) in the KBr press machine (model Mp-15) at 5 kg/cm^2 pressure for 2 min. After

taking background scan, samples were analyzed at 400-4000 cm^{-1}. FTIR direct-transmittance spectroscopy (KBr) was used to indicate the degree to which oxygen groups were removed and the IR absorption of water from the air was mostly eliminated. Each measurement was repeated in triplicates to minimize the error.

Chicken embryo model, autopsy and morphometry

As described in chapter 2

Bone and cartilage staining

Control and treated (TiO_2 NPs) embryos were processed for Alizarine-alcian blue staining (Lamb *et al.*, 2003). Briefly, skin and viscera was removed and embryos were fixed in 96% ethanol for 3 days followed by acetone for 2 days. Later, embryos were then rinsed in ethanol for 1–2 h and stained with Alizarine-alcian blue stain (0.015% Alcian blue, 0.005% Alizarin red in 70% ethanol, 20% acetic acid and 10% dH_2O) at 37ºC for 4 h. Embryos were rinsed in ethanol and running tap water for one hour each and muscles were cleared in an aqueous solution of 1% potassium hydroxide. De-staining of embryos was done in a graded series of glycerol/potassium hydroxide (20% glycerol/0.8% KOH, 50% glycerol/ 0.5% KOH and 80% glycerol/0.2% KOH respectively) and stored in 100% glycerol.

Inductively coupled plasma optical emission spectroscopy (ICP-OES)

The treated and control eggs after 4 days of incubation were opened and embryos digested overnight at 40^{o}C in 6 ml of conc. nitric acid and 3 ml of hydrogen peroxide. Then they were heated in an oven to 110^{o}C for 2 hrs, allowed to cool till room

temperature and diluted with 11 ml of dH_2O. The concentrations of nanosized particles in the embryo were quantified by ICP-OES. (Bryszewska *et al.*, 2009)

Shell-less culture and dosing

In a separate set of experiment, procured eggs were incubated for 60 h in standard conditions and later were explanted into shell-less culture as per Dugan *et al.* (1991) The embryos were divided into four groups of three eggs each viz control (50 µl PBS), positive control (50 µl of 50 µM $CdCl_2$), TiO_2 NPs treated (50 µl of 10 µg/ml) and bulk (50 µl of 10 µg/ml). Dosing was done directly on blastodisc using a micropipette and embryos were incubated until 4 h or 24 h.

Autopsy, RNA isolation and qPCR study

At the end of incubation, embryonal discs (HH 17; whole embryo) were transferred in RNA later solution (Ambion Inc., USA). For HOXD13, limb buds of 4 day old control and treated embryos were stored in RNA later solution. Total RNA was isolated using TRIzol reagent (Invitrogen, California, USA), cDNA was synthesized by reverse transcription of 1 µg of total RNA using iScript cDNA Synthesis kit (BIORAD, California, USA), detailed methodology is described in chapter 1. Quantitative RT-PCR was performed using SYBR Select Master Mix (Applied Biosystems) in QuantStudio12K (Life Technologies) real-time PCR machine with primers to detect selected messenger RNA (mRNA) targets. The PCR mixture contained 1 µl of cDNA, 5 µl of 2× SYBR Green PCR Master Mix and 10 nmol of each gene-specific primer in a final volume of 10 µl. All the PCRs were performed under following conditions: 2 min at 50 °C, 2 min at 95 °C, and 40 cycles of 15 s at 95 °C and 1 min at 60 °C in 96-well optical reaction plates (Applied Biosystems, USA). The specificity of amplicons was

verified by melting curve analysis (60 to 95 °C) after 40 cycles. The relative mRNA expression levels were normalized against expression levels of GAPDH for each sample and analyzed using $2^{-\Delta\Delta CT}$ method (Livak & Schmittgen, 2001). Primers used for this study are listed below:

Gene	Gene Name	Primer Sequence (5'-3')
GAPDH	Glyceraldehyde 3-phosphate dehydrogenase	F:-ACTGTCAAGGCTGAGAACGG R:-ACCTGCATCTGCCCATTTGA
HOXD13	Homeobox D-13	F:-TCTGGCTAATGGCTGGAACG R:-ATCTCGGGCTGGTTTAGTGC
CTNNB1	ß-catenin	F:-GTCCTGTATGAGTGGGAGCA R:-GTTTCGGGGAACATAGCAGAA
PITX2	Paired-like homeodomain 2	F:-CGATGAGTTGCATGAAGGAC R:-AGGAGGAAGGTGAGGAGGAG
LEF1	Lymphoid enhancer-binding factor 1	F:-TCACCTACAGCGATGAGCAC R:-TATCAGGAGCTGGAGGATGC
WNT11	Wingless-type MMTV integration site family, member 11	F:-TTCATCTTTGGCCCTGAATC R:-AGCTCGATGGATGAGCAGTT
PRKCA	Protein kinase C	F:-ACAACCAGGACCTTCTGTGG R:-TCTCGTAGAGCAGCACTCCA

CAMK2D	Calcium/calmodulin-dependent protein kinase II delta	F:-GCCAATCCACACCATTATCC R:-CCATCCATGTACTGCGTGAG
ROCK1	Rho-associated, coiled-coil containing protein kinase 1	F:-TGACTGGTGGTCAGTTGGAG R:-TAGAGATCTCGTTGTCATCAGG
ROCK2	Rho-associated, coiled-coil containing protein kinase 2	F:-GACTGGTGGTCCGTAGGAGT R:-GCAGTCTCTCGGATGTTGTC

Somite development

To examine the effects of TiO_2 NPs treatment on the appearance and growth of somites, chicks were treated with 50 µL 50 µM $CdCl_2$, 10 µg/ml TiO_2 NPs or 10 µg/ml TiO_2 bulk in shell-less culture mentioned above at 60 h (6 embryos per group). They were harvested 24 hours later, dissected from their membranes, and inspected using the dissecting microscope to count somite numbers.

Statistical analysis

Data analysis was carried out by unpaired Student's t-test or one way analysis of variance (ANOVA) using Graph Pad Prism 6.0 (CA, USA). Differences between control and treatment groups were deemed to be significant when $P \leq 0.05$.

RESULTS

Spectroscopic characterization

Comparative FT-IR spectra (400-4000 cm^{-1}) of native albumen and TiO_2 NPs + albumen depicting amide A (around 3400 cm^{-1}), amide B (about 3090 cm^{-1}), amide I and II (region between 1600-1700cm^{-1}) domains are shown in Figure 5.1a. The broad peak at 3591 and 3434 cm^{-1} in the amide A region of native albumen corresponds to the H-O-H asymmetric and symmetric stretching respectively, TiO_2 NPs + albumen recorded a shift in H-O-H stretching peak to 3478 cm^{-1}. Also, a shift in peak from 2071 cm^{-1} (in albumen) to 2083 cm^{-1} (TiO_2 NPs + albumen) was recorded. The amide I and II secondary fingerprint regions (in albumen) recorded two peaks at 1651 cm^{-1} and 1642 cm^{-1} but in TiO_2 NPs + albumen a peak was recorded at 1641 cm^{-1}. A peak in the amide III region was recorded at 1243 cm^{-1} in albumen whereas, TiO_2 NPs + albumen recorded a shift to peak 1551 cm^{-1}. Also, peaks at 1457 and 1451 cm^{-1} in albumen and TiO_2 NPs + albumen respectively are due to $–CH_2$ scissoring vibration whereas, a peak at 675 cm^{-1} in TiO_2 NPs + albumen corresponds to Ti-O vibrational mode of TiO_2 NPs. Results obtained in deconvoluted Gaussian fitted spectra (Figure 5.1b, 5.1c) and integrated peak areas of secondary-derivative structure element (Figure 5.1d and Table 5.1) showed that albumen was mainly composed of side chain (1610 cm-1, 20.93%) inter or intramolecular β sheet (1621-1629 cm^{-1}, 39.11%) closely followed by α helices (1664 cm^{-1}, 13.94%) with minor proportions of β turns (1681 cm^{-1}, 11.95%) and β sheet (1695 cm^{-1}, 10.76%). After interaction with TiO_2 NPs, a decrease in side chain (1607 cm^{-1}, 4.11%), β turns (1681 cm^{-1}, 10.31%) and β sheet (1695 cm^{-1}, 8.81%) and an increase in inter or intramolecular β sheet (1621cm^{-1}, 53.39%) and α helices (1661 cm^{-1}, 17.46%) was recorded.

ICP-OES analysis of embryos

After 4-days of TiO_2 NPs treatment, the contents of Ti in the chick embryo were measured by ICP-OES. Significantly high levels of Ti was detected (3 times increase) in embryos of eggs treated with 10 µg/ml TiO_2. But, higher dose (100 µg/ml) accounted for a moderate non significant content of Ti in embryos (Figure 5.2).

Deformity

Control and TiO_2 NPs treated chick embryos were examined as per Hamburger-Hamilton standard which revealed presence of flexed limbs at 10 and 25 µg/ml doses (Figure 5.3). Also, omphalocele (ventral body wall defect) was observed at 10 µg/ml dose only. These deformities were not seen at 50-1000 µg/ml doses. Confirmation of flexed limbs of 10 and 25 µg/ml treated embryos was obtained by alcian blue- alizarine red staining (Figure 5.4).

Expression of Wnt signaling genes

RT-PCR analysis was performed to assess the effect of TiO_2 NPs on expression of some key genes of canonical (CTNNB1, PITX2 and LEF1), non-canonical Wnt/Ca^{2+} (WNT11, PRKCA and CAMK2D) and Planar Cell Polarity pathway (ROCK1 and ROCK2) associated with Wnt signaling. Expression levels of CTNNB1, PITX2 and LEF1 were down regulated significantly (Figure 5.5) in embryos treated with TiO_2 NPs (10 µg/ml). Similar decrement was also observed in cadmium treated embryos, whereas, TiO_2 bulk treatment did not account for any significant change. Expression levels of key genes of non-canonical Wnt/Ca^{2+} Wnt signaling viz. WNT11, PRKCA and CAMK2D showed significantly lowered expression levels following TiO_2 NPs and cadmium treatment (Figure 5.5). However, the TiO_2 bulk treatment showed non-significant changes in the

expression levels of the said genes. mRNA expression of key genes of Planar Cell Polarity pathway viz. ROCK1 and ROCK2 showed moderately significant decrement in ROCK1 expression and non significant decrement in ROCK2 expression following TiO_2 NPs or cadmium treatment (Figure 5.5). TiO_2 bulk treatment accounted for a non significant increment in expression of ROCK1 and ROCK2 genes. Expression levels of HOXD13 showed significantly lowered expression levels following TiO_2 NPs or cadmium treatment, whereas, the TiO_2 bulk treatment showed non-significant changes (Figure 5.6).

Somite development

60 h old embryos were treated with 10 µg/ml TiO_2 nanoparticles and possible discrepancy in somite numbers was studied after 24 h. It was observed that 10 µg/ml dose accounted for 20% decrement in the number of somites after 24 h (Figure 5.7).

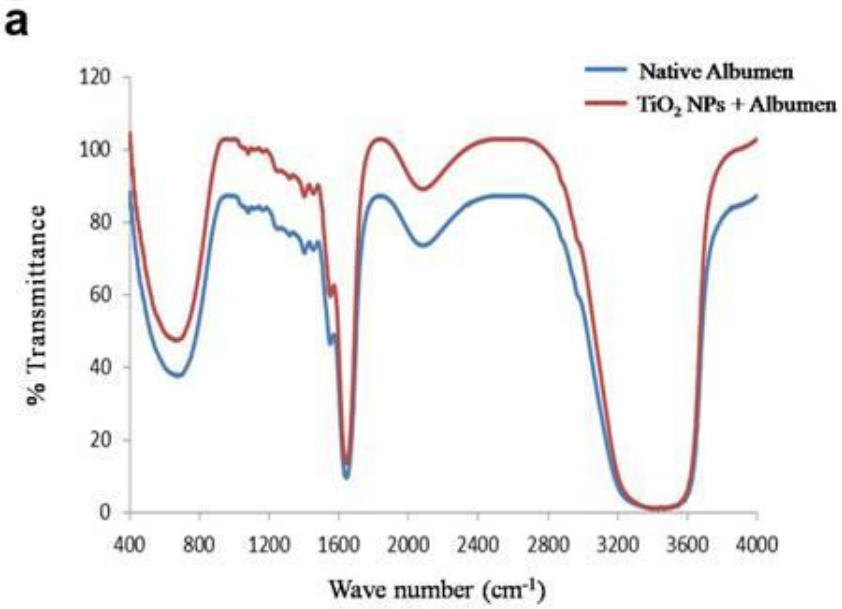

(Legend on the next page)

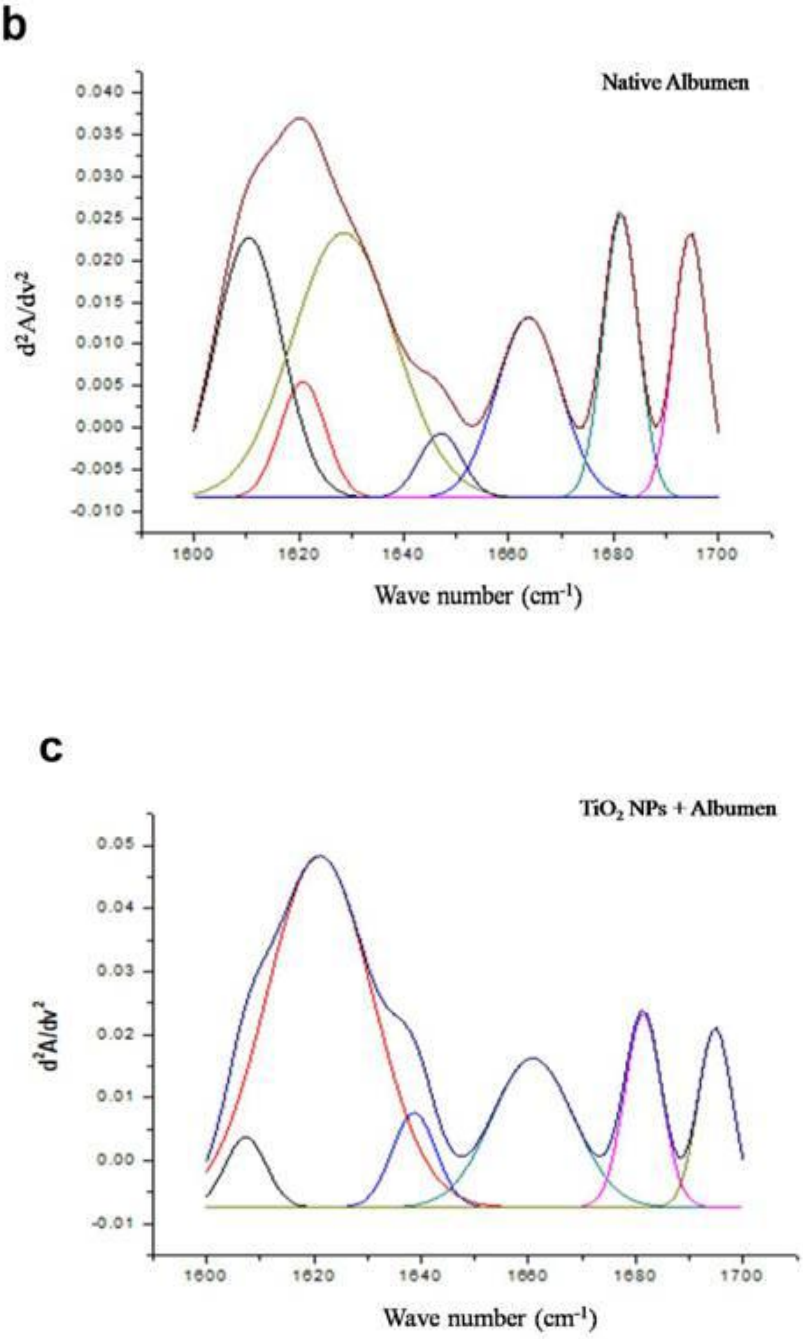

(Legend on the next page)

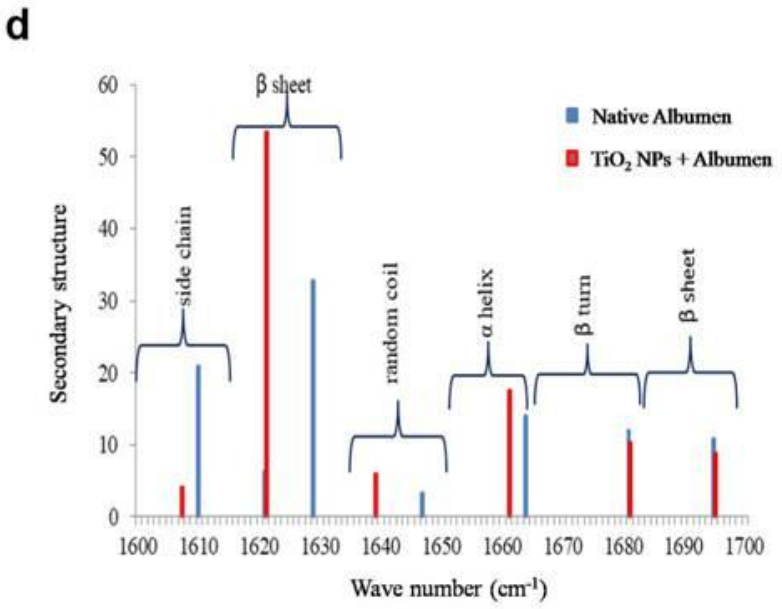

Figure 5.1: FTIR spectra of native egg albumen and TiO_2 NPs + Albumen. (a) Entire spectral range from 400-4000 cm^{-1}; (b, c, d) Gaussian curve fitting of secondary derivative of Native Albumen and TiO_2 NPs + Albumen with Comparative Secondary structure elements from FTIR spectra.

Table 5.1: Percentage of secondary structure components in Native Albumen and TiO_2 NPs + Albumen

	% secondary structure					
	Side chain	β sheet	Random coil	α helix	β turn	β sheet
Native Albumen	20.93	39.11	3.30	13.94	11.95	10.76
TiO_2 NPs + Albumen	4.11	53.39	5.93	17.46	10.31	8.81

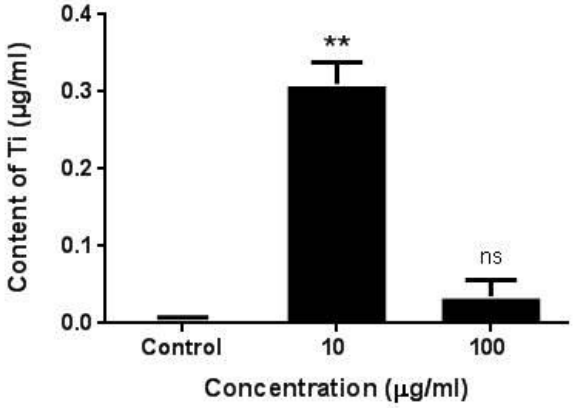

Figure 5.2: Concentration of Ti in embryos of control and TiO_2 NPs-treated group (4 day old) by ICP-OES. The data are expressed as Mean±SD. Statistical analysis was done by one way ANOVA, **p< 0.01, ns- non significant.

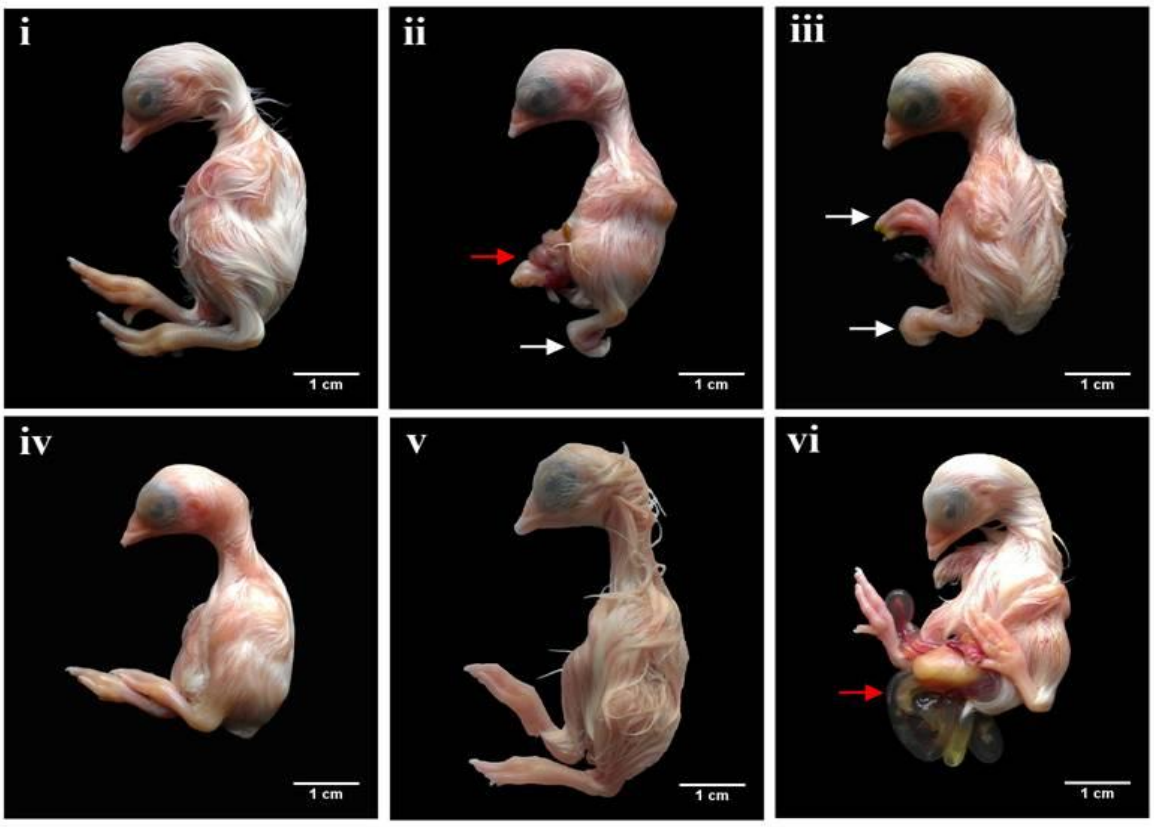

Figure 5.3: Chicken-embryo development after 19 days of incubation, i-control, 10-100 µg/ml TiO_2 NPs-treated groups (ii,iii,iv), 10 µg/ml TiO_2 Bulk (v) and 10 µg/ml cadmium chloride (vi), (Scale bar: 1 cm). Embryos treated with 10 µg/ml TiO_2 NPs (ii) exhibits omphalocele (red arrow) & flexed limbs (white arrow).

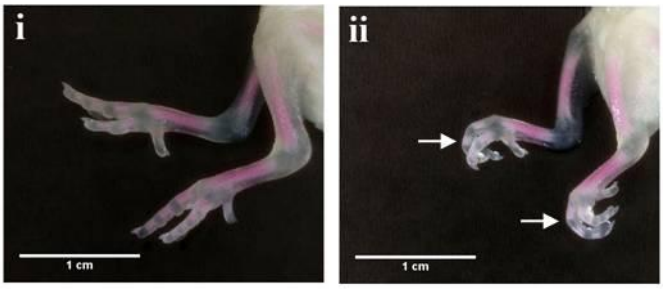

Figure 5.4: Photographs showing endoskeleton (bone and cartilage) of 19-day-old chick embryos, control (i) and TiO_2 NPs–treated (ii) stained with Alizarin red S and alcian blue staining. TiO_2 NPs treated (10µg/ml) embryos exhibits flexed digits (arrow).

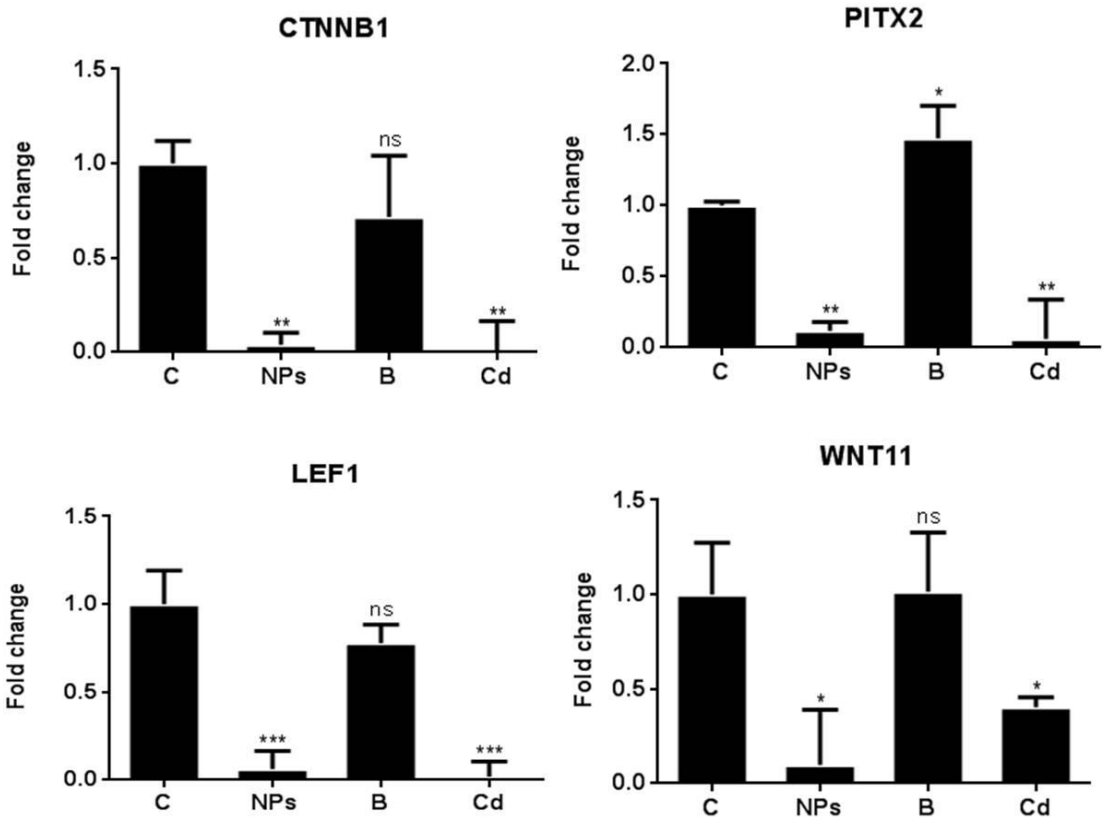

(Legend on the next page)

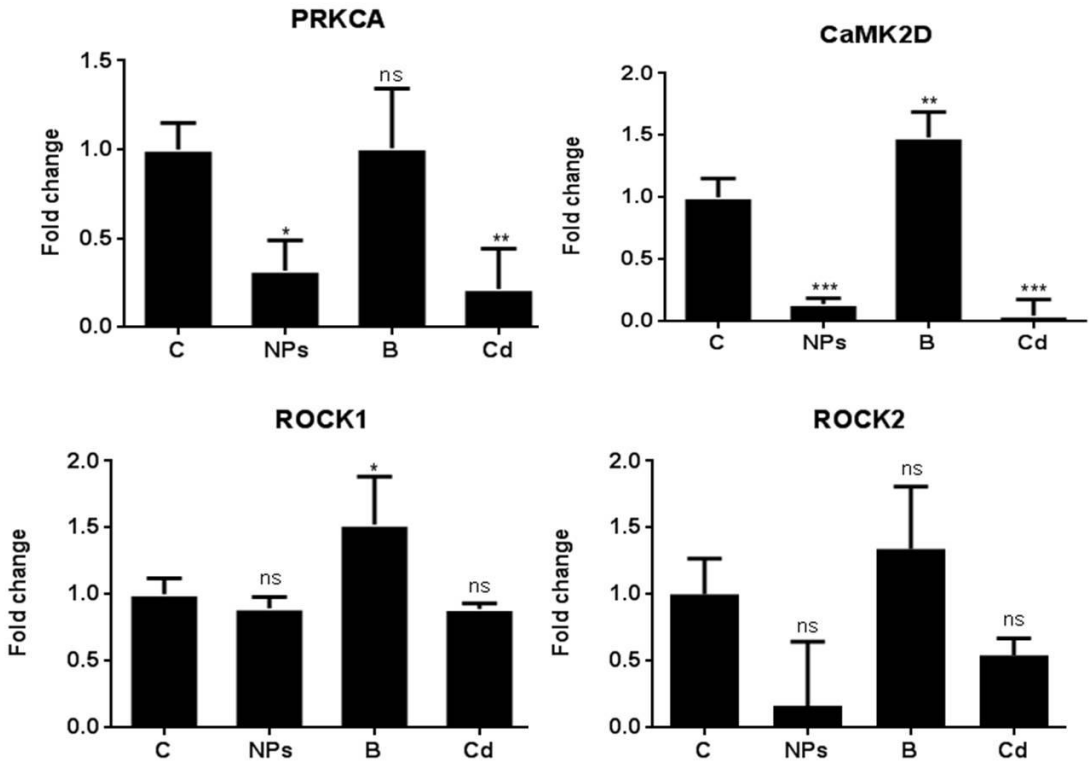

Figure 5.5: Expression of Wnt signaling pathway-related genes in TiO_2 NPs-treated chicken embryos. The expression of Wnt signaling pathway-related genes including CTNNB1, PITX2, LEF1, WNT11, PRKCA, CAMK2D, ROCK1 and ROCK2 was analyzed using reverse transcription polymerase chain reaction (RT-PCR) in control and TiO_2 NPs-treated embryos (n=3), 4 h after treatment in shell-less at 60 h. The data are expressed as Mean±SD. Statistical analysis was done by one way ANOVA followed by Dunnett's test. *$p < 0.05$, **$p< 0.01$, ***$p< 0.001$, ns=non significant. C- control, P-placebo, B- TiO_2 Bulk (10 µg/ml), Cd- cadmium chloride (10 µg/ml).

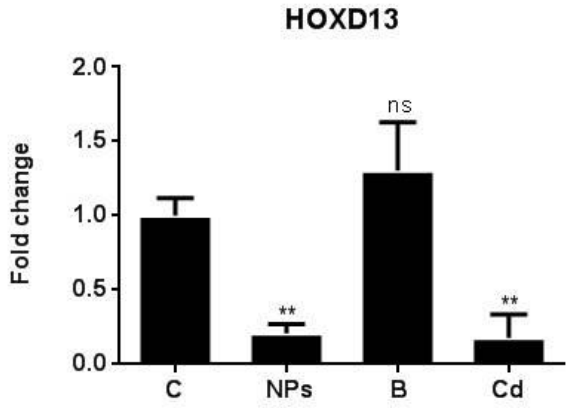

Figure 5.6: Expression of limb development gene HOXD13 in TiO_2 NPs-treated chicken embryos. The data are expressed as Mean±SD. Statistical analysis was done by one way ANOVA followed by Dunnett's test. **p< 0.01, ns=non significant. C- control, P-placebo, B- TiO_2 Bulk (10 µg/ml), Cd- cadmium chloride (10 µg/ml).

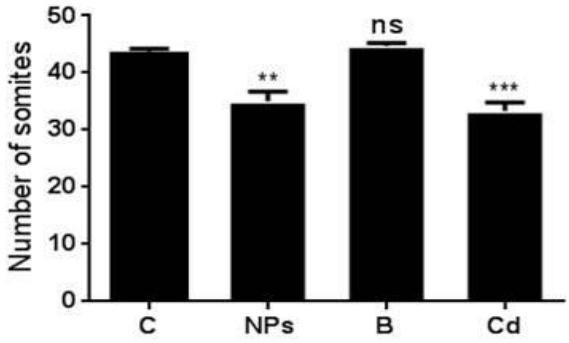

Figure 5.7: Somite numbers in control and TiO_2 NPs-treated embryos 24 h after treatment in shell-less culture (HH-23). There is a reduction in the number of somites in TiO_2 NPs-treated embryos as compared to the control embryos. The data are expressed as Mean±SD. Statistical analysis was done by one way ANOVA followed by Dunnett's test. *p < 0.05, **p< 0.01, ***p< 0.001, ns=non significant. C- control, P-placebo, B- TiO_2 Bulk (10 µg/ml), Cd- cadmium chloride (10 µg/ml).

DISCUSSION

Nanomaterials have been reported to interact with protein molecules in unique ways and form a 'protein corona' that alters its physicochemical identity in physiological environment thus affecting its bio-distribution, kinetics and subsequent toxicity (Walkey & Chan, 2012). Egg albumen is reservoir of protein in an avian egg that meets the nutritional requirements of a developing embryo. Besides egg shell, shell membrane and chorioallantoic membrane; egg albumen also regulates the trafficking of exogenous elements by acting as a natural biological barrier (Willems *et al.*, 2014). TiO_2 NPs + albumen recorded a shift in H-O-H stretching peak to 3478 cm^{-1} confirming interaction between TiO_2 NPs and albumen. Further a shift in peak from 2071 cm^{-1} (in albumen) to 2083 cm^{-1} (TiO_2 NPs + albumen) is attributable to interaction between C-O and amide groups of amino acids present in albumen. Peaks observed in the amide I and II secondary fingerprint region (in albumen) at 1651 cm^{-1} and 1642 cm^{-1} are attributable to C=O stretching and H-O-H bending respectively. However, a minor shift in C=O stretching and depletion of H-O-H bending (at 1641 cm^{-1}) was possibly on account of electrostatic interaction due to Vander Waal forces taking place between albumen and TiO_2 NPs. Peak in amide III region (at 1243 cm^{-1}) in albumen occurs due to N-H bending and C-N stretching of amino groups but, TiO_2 NPs + albumen recorded a shift (at 1551 cm^{-1}) from amide III to amide II region. This shift also portrays major conformational changes in secondary components (α helices and β sheet) of proteins possibly due to their interaction with TiO_2 NPs. Fourier-self deconvolution approach was employed to assess secondary conformational changes in amide I and II region. Venyaminov and Kalnin (1990) had reported that amide peak at 1610±4 corresponds to NH bending of $CO\text{-}NH_2$

bond in glutamine. In our study, amide peak at 1610 cm^{-1} in TiO_2 NPs + albumen indicates possible deformity of glutamate in egg albumen. Role of glutamate in nutrition and metabolism is well reported (Brosnan & Brosnan, 2013) and hence impact of structurally altered glutamate on developing chicken embryo is postulated herein. Further, an increase in β sheet and α helices in TiO_2 NPs + albumen are possibly due to TiO_2 NPs mediated conformational changes, formation of aggregates or amyloids with protein moieties in egg albumen. Interaction of TiO_2 NPs with egg albumen prompted us to assess its impact on embryonic development using chicken egg as a model. HH-scoring for embryonic deformities revealed omphalocele and flexed limbs at lower doses (10 and 25 µg/ml) of TiO_2 NPs whereas, no deformity was observed at higher doses. This is a non-classical toxicological response wherein, the lower doses (10 and 25 µg/ml) were able to manifest more mortality and developmental deformity than higher doses.

The nanoparticles are known to cross biological barriers like the blood brain barrier and blood placenta barrier (Rollerova *et al.*, 2015), and the results obtained herein indicate that the nanoparticles could cross the barriers within an avian egg and reach the embryo. ICP-OES studies confirmed presence of higher levels of TiO_2 NPs in the embryonic tissue at the lower dose (10 µg/ml). This study demonstrated that TiO_2 NPs (10 µg/ml) treatment to chicken embryos at H-H stage 16 to 17 (60 hours of incubation) induced omphalocele. Omphalocele is a ventral body wall defect and is accompanied by herniation of midgut into the abdominal cavity, failure in fusion of the anterior abdominal wall with 1/3000 frequency of occurrence in human population (Doi *et al.*, 2011). Teratogenic agents such as cadmium (Thompson & Bannigan, 2007), specific radiations (Pampfer & Streffer, 1988), fungal toxins (Wangikar *et al.*, 2004) etc. are known to

induce omphalocele in various animal models. However, no known nanomaterials have been reported to induce omphalocele and this is the first report that investigates TiO_2 NPs induced omphalocele in chicken embryo model. Wnt signaling pathway has been implicated in various events of embryonic development such as cell differentiation, survival, migration, proliferation, adhesion and somite formation (Doi *et al.*, 2010). Canonical Wnts relay their signal via ß-Catenin pathway that control cell fate determination (Doi *et al.*, 2010). Whereas, the non-canonical Wnt signaling either through Wnt/Ca^{2+} pathway or planar cell polarity pathway that controls cell adhesion and movement (Doi *et al.*, 2010). Results obtained herein were compared with cadmium induced omphalocele chicken embryo model (Thompson & Bannigan, 2007). PITX2, a bicoid-type homeodomain transcription factor, has known to be regulated by ß-Catenin dependent Wnt pathway (Kioussi *et al.*, 2002). In the Wnt/β-Catenin pathway, the accumulation of ß-Catenin in the nucleus converts DNA-binding factor, lymphoid enhancing factor-1 (LEF1), to a transcriptional activator and is regulated through direct physical interaction with PITX2 and ß-Catenin (Vadlamudi *et al.*, 2005). In this study, downregulation in expression levels of CTNNB1, PITX2 and LEF1 after TiO_2 NPs treatment could be a key factor in the disruption of somite myogenesis by inhibiting Wnt/β-Catenin pathway. It has been postulated that cells from somites migrate into the parietal layer of lateral plate mesoderm (LPM) to assist in forming the lateral body folds (Burke & Nowicki, 2003). PITX2 is known to regulate cell survival and its inactivation in mice is reported to result in the apoptosis of first branchial arch myogenic cells (Shih *et al.*, 2007). Downregulation of PITX2 in this may induce abnormal apoptosis in the somite and LPM and interfere with the movement of the lateral body wall folds ventrally. These

results of cell death in somite are in agreement with the somite count obtained in our study, which showed decrement in the number of somites in TiO_2 NPs treated group. WNT11, a member of the noncanonical Wnts, is an important epithelialization factor acting on the dermomyotome and PRKCA and CaMK2D control actin-cytoskeleton organization and cell contractility, and thereby contribute to several physiologic processes, including tissue closure (Doi *et al.*, 2010; Geetha-Loganathan *et al.*, 2006). Previous studies have implicated PRKCA and CaMK2D (activated by WNT11) in the regulation of cell-cell adhesion molecules (CAMs) such as cadherins, which bind directly to β-Catenin, resulting in a linkage between E-cadherin and actin filaments and reinforce the cell-cell junctional connection (Ozaki *et al.*, 2007). In this study, downregulation in expression levels of WNT11, PRKCA and CaMK2D after TiO_2 NPs treatment may interfere with actin-cytoskeleton organization, cell movement and cell adhesion, disrupting noncanonical Wnt/Ca^{2+} signaling and causing omphalocele. Rho kinase (ROCK) belongs to a family of serine/threonine kinases that are involved in the regulation of various cellular functions such as contraction, adhesion, migration, proliferation and apoptosis, thereby, contribute to several physiological processes, including tissue closure during embryonic development. ROCK1 and ROCK2 mediate signaling from Rho to the actin cytoskeleton in the Wnt non-canonical pathway (J. Shi & Wei, 2007). ROCK1 knockout (KO), ROCK2 KO, and ROCK1/2 double heterozygous mice exhibit omphalocele phenotype due to disorganization of actin filament in the epithelial cells of the umbilical ring (Shimizu *et al.*, 2005). Disturbance in the actin cytoskeleton integrity via ROCK inhibition can initiate events that commit a cell to apoptosis (J. Shi & Wei, 2007). Downregulation of ROCK genes in the TiO_2 NPs treated

group may cause disruption of actomyosin assembly, migration of lateral embryonic folds by altering actin and β-catenin distribution in periderm, resulting in the failure of closure of the umbilical ring and causing omphalocele. Several genetically-modified animals that have been reported to display abnormalities in the body wall region had accompanying limb deformities (Matsumaru *et al.*, 2011). *Hox* genes are important regulators of limb pattern in vertebrate development, HOXD13 misexpression in the hindlimb results in shortening of the long bones, including the femur, the tibia, the fibula and the tarsometatarsals (Goff & Tabin, 1997). In our study, significantly lowered expression of HOXD13 in TiO_2 NPs treated embryos corroborate with the observed omphalocele. Cadmium is known to use Ca^{2+} ion channels and membrane transporters to gain access into target cells of mammalian organisms and disrupt lateral plate mesoderm and induce apoptosis (Thompson & Bannigan, 2007). This mechanism is similar to one proposed for free radicals, where the radical becomes affixed to or within the cell membranes (Van Dorp *et al.*, 2010) and TiO_2 NPs are known to cause damage by producing free radicals (Shukla *et al.*, 2013). Hence, TiO_2 NPs may also be causing omphalocele by disrupting lateral plate mesoderm, somite myogenesis and inducing apoptosis as also evidenced by the above gene expression studies. The possible mechanism of TiO_2 NPs induced omphalocele and flexed limbs is given in figure 5.8.

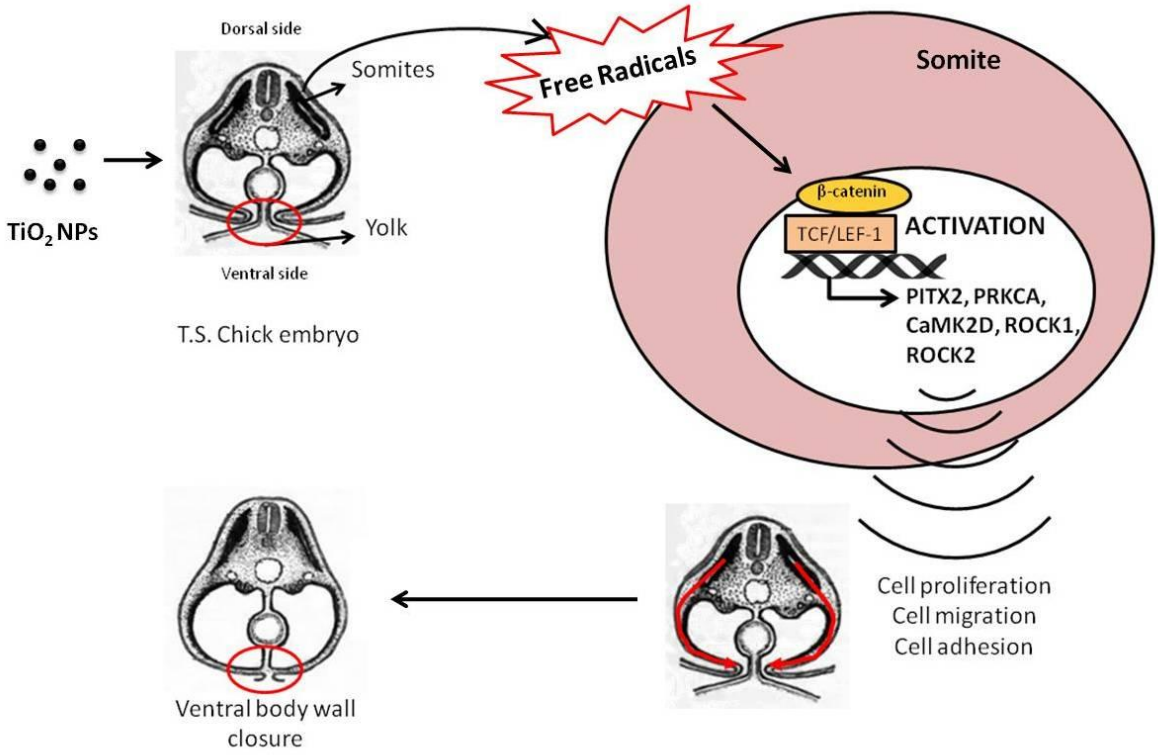

Figure 5.8: The possible mechanism of TiO_2 NPs induced omphalocele and flexed limbs

SUMMARY

Nanometal oxides witness a wide range of biomolecules in a physiological environment that can alter their behavior and responses. Hence, the aim of the present study was to evaluate the interaction of egg albumen with TiO_2 NPs and its subsequent impact on an avian embryo. TiO_2 NPs were found to interact with egg albumen as evidenced by changes in their proteinic secondary structure. TiO_2 NPs were also dosed in the airspace of fertilized eggs of *Gallus gallus domesticus* and incubated until 19 days. The malformations (omphalocele and flexed limbs) caused could be because of the interactions of TiO_2 NPs with egg albumen allowing TiO_2 NPs to traverse the biological barriers (shell membrane and CAM) within chicken egg as confirmed by ICP-OES studies and affect the growth and development of embryos. Wnt signaling plays an important role in the ventral body wall formation. Downregulation of genes involved in Wnt signaling (CTNNB1, PITX2, LEF1, WNT11, PRKCA, CaMK2D, ROCK1 and ROCK2) leads to the distruption of somite myogenesis which interfers with the movement of the lateral body wall folds ultimately causing omphalocele.